DISTINCT ION POPULATION IN THE POLAR CUSP: POSSIBLE SIGNATURE OF TRANSIENT RECONNECTION

C. P. Escoubet[1], M. F. Smith[2], J. M. Bosqued[3]

[1]Space Science Department of ESA/ESTEC, Noordwijk, The Netherlands
[2]Laboratory for Extraterrestrial Physics, NASA/GSFC, USA
[3]Centre d'Etude Spatiale des Rayonnements, Toulouse, France

ABSTRACT

Observations of ion energy dispersion are a common feature of the polar cusp. Normally these dispersions show a continuous decrease in energy. However, they occasionally show step-like features in the dispersion. On 15 October 1981 Dynamics Explorer 2 (DE 2) crossed the polar cusp at 1015 MLT and observed three distinct ion populations as the spacecraft moved poleward. These three populations had peak-flux energy around 2.7 keV, 850 eV and 360 eV. The first step coincided with a rotation of the flow; the flow being directed westward on the equatorward edge, poleward in the center and eastward on the poleward edge. The second and third steps showed a flow directed principally poleward. Furthermore, the magnetic and electric perturbations in the first step are well fitted by an elongated FTE footprint model. These results suggest that three consecutive Flux Transfer Events (FTEs) have injected solar wind plasma into the ionosphere forming the polar cusp. The small latitudinal size of these FTE footprints ($\sim$ 40 km) and their short recurrence rate (3 and 6 min) would be consistent with an intermittent reconnection taking place at the subsolar point on a short time scale.

Keywords: magnetic reconnection, flux transfer event, polar cusp, ionospheric convection.

1. INTRODUCTION

Since the first observations of precipitating particles in the polar cusp (Ref. 1) dispersions in energy of the ions have often been observed. These dispersions arise from the convection electric field acting as a velocity filter on the particles from the injection point to the observation in the ionosphere (Refs. 2,3). Sometimes the precipitation of the ions does not show a monotonic decrease or increase of the energy but a more complex pattern like a butterfly signature (Ref. 1); a dispersion associated with a diffuse precipitation (Refs. 4,5); a double dispersion (Ref. 6); a change in the slope of the dispersion (Ref. 7); jumps in energy (Ref. 8); or narrow arcs of ions superimposed on the dispersion (Ref. 9). These distortions of the dispersion could be due to a change in the convection electric field caused by a variable ionospheric conductivity (Ref. 10), or by a variable reconnection rate which would drive a variable electric field in the ionosphere. For example, intermittent reconnection may be responsible for the appearance of transient and localized bursts in the ionospheric flow (Ref 11).

In addition, another cause of distortion of the dispersion could be the successive injections of short-lived sources resulting in temporal rather than spatial dispersion (Ref. 12). A Flux Transfer Event (FTE) (Ref. 13) might be seen as a short-lived and moving source which injects particles into the polar ionosphere (Refs. 14,15,16). With an average scale size of the ionospheric FTE footprint of 300 km (Ref. 17) and a recurrence time $\sim$ 8 min (Ref. 18), the probability of observing the signature of two FTEs is 40% around local noon (Ref. 16). However if reconnection takes place on shorter time scales, the probability to observe more than one FTE footprint with a polar orbiting spacecraft increases strongly.

In this paper we report a DE 2 cusp crossing during which the observed ion dispersion consists of three distinct energy steps. We interpret these observations as three successive FTEs, reconnected on the dayside magnetosphere at a time interval of 3 and 6 min, which inject particles and move poleward into the polar cap.

2. OBSERVATIONS

On 15 October 1981 the DE 2 satellite crossed the northern polar cusp at an altitude of 780 km around 1015 MLT (Figure 1). The IMF, obtained by the ISEE-3 spacecraft (courtesy of NSSDC) was southward with Bx, By, and Bz components equal to 0, -1.5 and -7 nT respectively. Panels a and b of Figure 1 show the energy-time spectrograms of the precipitating electrons and ions respectively (pitch-angles of 10° and 18°) obtained by the Low Altitude Plasma Instru-

Proceedings of the 26th ESLAB Symposium – Study of the Solar-Terrestrial System, held in Killarney, Ireland, 16–19 June 1992 (ESA SP-346, September 1992)

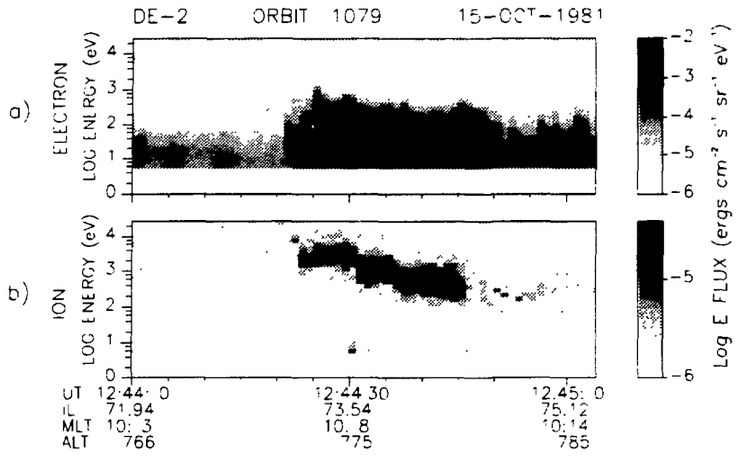

Figure 1. Data from DE-2 satellite on 15 October 1981. Energy-time spectrograms of the precipitating electrons (a) and ions (b) between 5 eV and 27 keV.

ment (LAPI) (Ref. 19). The aim of this paper is not to distinguish the cusp and cleft regions but to study the mechanism of entry of solar wind particles in the dayside magnetosphere and therefore we will consider the cusp and cleft regions together. Using the definition from Newell and Meng (Ref. 20), the cusp/cleft region is located between 12:44:24 UT (73.2° ILAT) and 12:44:46 UT (74.3° ILAT). The high energy electrons above 35 keV (not shown here) were isotropic after 12:44:16 UT and throughout the polar cap, indicating that the magnetic field lines were probably open. The ion data (panel b) show three distinct energy steps with decreasing energy toward the pole. The first step (region A), observed from 12:44:24 UT to 12:44:31 UT, was characterized by a peak-flux energy around 2.7 keV (Figure 2a). The second step (region B), observed from 12:44:31 UT to 12:44:36 UT, had a peak-flux energy around 850 eV and the third step (region C), from 12:44:36 UT to 12:44:46 UT, had a peak-flux energy around 360 eV. The boundary between region A and B has been defined as the point where the peak-flux energy decreased from 2 keV to 850 eV (Figure 2a) and the boundary between region B and C by the point where the peak-flux energy decreased from 640 eV to 270 eV. The region A, where the highest energy ions precipitated, shows an intense precipitation of electrons (Figure 1a) with an electron burst at 12:44:26 UT.

The east-west (Bz) and north-south (Bx) components of the magnetic field (Figure 2b and 2c respectively), obtained from the Magnetometer (MAG-B) (Ref. 21), showed the largest variations in the region A: the Bz component increased by 150 nT on the equatorward side of region A then rapidly decreased by 200 nT simultaneously with the electron burst on Figure 1a. The Bz component then remained approximately constant around 125 nT for $\sim$ 3 s in the center of region A before decreasing again strongly by 175 nT on the poleward side of region A. The Bx component decreased by almost 200 nT from the equatorward boundary to the center of region A, then was approximately constant for 2 s and increased by 130 nT on the poleward side of region A. In regions B and C variations in Bz and Bx components were smaller than those detected in region A, excepted at the poleward boundary of region C, where Bz decreased by 200 nT and Bx by 130 nT.

The north-south component of the electric field (Ex), obtained from the Vector Electric Field Instrument (VEFI) (Ref. 22), is shown on Figure 2d. Note the very good correlation between Ex and Bz components (R=0.96 between 12:44 UT and 12:45 UT) which gives an average conductivity $\Sigma p = 6.3$ mhos (Ref. 23). Positive (negative) values of the electric field are equivalent to a westward (eastward) convection velocity. The other component of the convection (north-south), obtained from the Retarding Potential Analyser (RPA) (Ref. 24), is shown on Figure 2e. Combining these two components, the convection was westward and poleward with a value around 500 m/s equatorward of the cusp region (before 12:44:23 UT). Then, on the equatorward boundary of region A, the flow became more westward with an increase of the westward component up to 750 m/s (Ex up to 50 mV/m) and abruptly rotated toward a poleward direction at 12:44:26 UT (simultaneous with the electron burst), taking a value around 1200 m/s. On the poleward side of region A, the convection decreased again around 600 m/s with an eastward and poleward direction which became purely eastward around 400 m/s near the boundary between region A and B. In regions B and C, the flow around 700 m/s was principally poleward directed with the east-west component fluctuating between 400 m/s and -400 m/s (Ex between 15 mV/m and -15 mV/m). Poleward of the cusp (after 12:44:50 UT), the convection was eastward and poleward with a value around 1200 m/s.

3. DATA INTERPRETATION

A continuous ion energy dispersion has generally been ex-

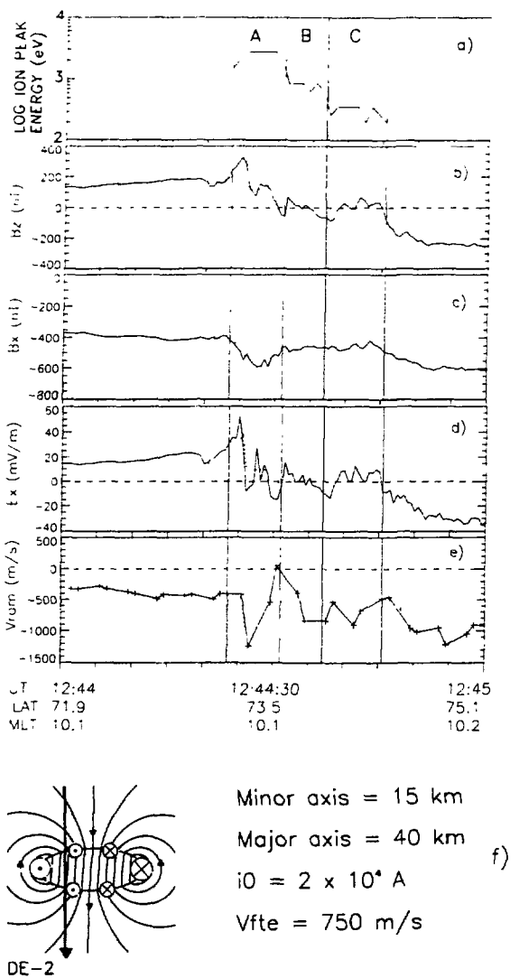

Figure 2. a) Energy of the ion flux peak. b) Measured (solid line) and computed (dotted line) perturbations of the east-west (cross-track) component of the magnetic field. c) north-south (along satellite trak) perturbations of the magnetic field. d) north-south convection electric field. e) north-south convection flow (negative values for a poleward flow). f) convection flow and field aligned currents (upward and downward on the left and right side of the tube respectivelly) of an elongated FTE footprint (from Wei and Lee [1990]). The best fit values of the major and minor axis, current i0 and flow velocity inside the tube are indicated on the right.

plained by particles injected continuously from a fixed source on the magnetopause and which have experienced a convective electric field on their way to the ionosphere (Ref. 3). A gradual varying convection would produce a change in the slope of the dispersion signature (Ref. 7) but not three distinct energy steps as those shown in Figure 1. On the other hand, a short injection would produce a temporal dispersion in the ionosphere (Ref. 12) and only one energy or a step in energy would be observed by a low-altitude spacecraft. To explain our staircase dispersion one must consider three short injections. The properties of these sources, short-lived, occurring for IMF-Bz< 0 and injecting particles into the polar ionosphere, are typical of FTEs (Refs. 25,15). Figure 3a sketchs a sequential view of the injection from one source (filled square) localized on the magnetopause. A time t_0, the particles (we will consider only ions but electrons are injected at the same time) leave the source and move along the magnetic field toward the ionosphere. If we assume that the duration of the injection is short compared to the travel time for the ions to reach the ionosphere then, at time t_1, the high energy ions (thick line) reach the ionosphere while the intermediate and low energy ions (line of intermediate thickness and thin line respectively) are still at higher altitude. At a time t_2 later, the intermediate energy ions reach the ionosphere and finally at time t_3, the low energy ions reach the ionosphere. Let now consider on Figure 3b that at each time t_i ($i = 1 - 3$) a new source S_i injects particles on neighbouring field lines of S_{i-1}. At time t_1, the high energy ions from S_0 reach the ionosphere (same as Figure 3a) and a new source S_1 injects particles. At time t_2, the intermediate energy ions from S_0 and the high energy ions from S_1 reach the ionosphere and S_2 injects particles. Finally at t_3, the low energy ions from S_0, the intermediate energy ions from S_1 and the high energy ions from S_2 reach the ionosphere while S_3 injects particles. If

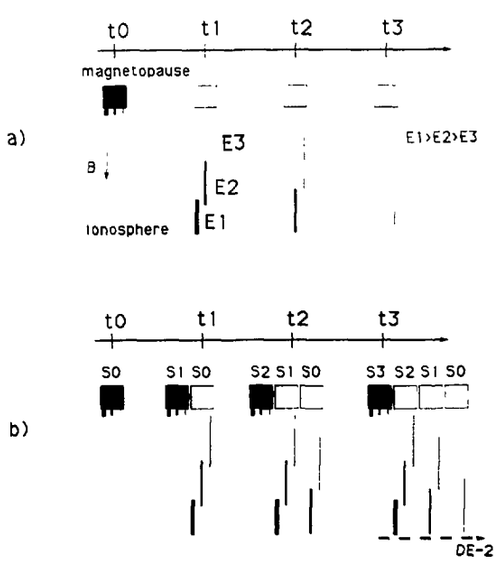

Figure 3. (a) Sequential sketch of one source injection into the polar ionosphere and (b) four consecutive source injections. The line segments represent the ions travelling along the magnetic field with the thickness of the line proportional to the ion energy.

we now consider that the sources are produced at the subsolar point by magnetic reconnection and then move poleward due to the magnetosheath flow (Figure 3c), a satellite moving toward the pole at low altitude will detect first the high energy ions (coming from S_2), then the intermediate energy ions (coming from S_1) and the low energy ions (coming from S_0). Practically, we do not observe, in each step one energy but a band in energy (Figure 1b) which means that the injection lasts for a certain period of time.

As proposed by Lockwood and Smith (26), an estimation of the beginning of the injection is given by the low energy cutoff of the ion flux: the lowest energy ions of each step were the first to be injected and this occurred when the FTE was reconnected near the subsolar point. If we assume a subsolar point around 16 R_E, the lowest energy ions of region A, B and C around 1.5 keV, 360 eV and 100 eV respectively gives the estimated time of reconnection of FTE S_2, S_1 and S_0 around 12:41 UT, 12:38 UT and 12:32 UT respectively. It follows that the time delay between the first FTE (S_0) and the second (S_1) is around 6 min and the delay between the second and the third (S_2) is around 3 min. These times are smaller than the average recurrence time of FTEs observed at the magnetopause (~8 min) (Ref. 18). However, the latitudinal width of the FTE footprints reported here (~40 km) is also smaller than the generally quoted width (~300 km) (Ref. 14). This would be consistent with an intermittent reconnection occurring on short time scale and producing small FTEs (Ref. 27).

Based on a recent model of ionospheric convection (Refs. 28,16) we have sketched the evolution of the convection due to three consecutive FTEs on Figure 4. At time t_1, we assume that the polar cap is in equilibrium (circular shape) and that an FTE is created in the morning sector due to the distortion of the geomagnetic field under IMF-By< 0 (Ref. 29). The flow which develops inside the FTE is first imposed by the tension of the field lines due to By component (eastward flow for By< 0) and then by the polar cap reaching a new equilibrium (poleward). As IMF-Bz component is greater than By with an angle between the IMF and the z axis ~ 12°, the flow inside the FTE would be more poleward than eastward (Ref. 30). The field aligned currents flowing on the edge of the FTE are upward on the eastward edge and downward on the westward edge. As reconnection goes on, the FTE expands and after a very short time the reconnection stops and the FTE starts being integrated into the polar cap and extending in longitude. At time t_2 another FTE is created equatorward around the same local time giving a new impulse to the flow. The flow expands poleward as the polar cap, disturbed by the new open flux appended to it, will try to reach a new equilibrium. Similarly, at time t_3 a third FTE is produced. At that time, if we consider a satellite trajectory around 10 MLT the convection would be westward and poleward equatorward of the FTEs (due to the return flow of the dusk cell) and poleward and eastward in the FTE footprints and throughout the polar cap, which is in good agreement with the data (bottom right panel).

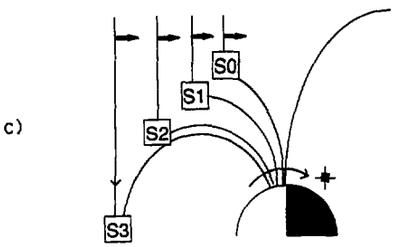

Figure 3. (c) Schematic process of intermittent reconnection wich produces a source S3 at the subsolar point (corresponding to time t_3 in Figure 3b). The previous sources S0, S1, and S2 have moved poleward along the magnetopause due to the magnetosheath flow (thich arrows).

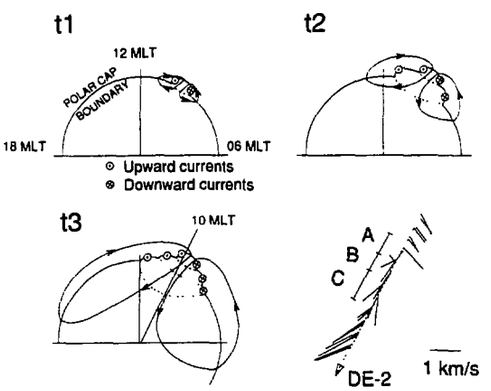

Figure 4. Evolution of the convection flow produced by three consecutive FTEs (adapted from Cowley et al. [1991]). The lower right panel shows the measured convection flow (deduced from Figure 2c and 2d).

To evaluate the current flowing on the edge of these FTEs, we have analysed in more details the magnetic and electric signatures of region A. We have chosen region A because the variations in electric and magnetic field are large (Figure 2), which means that the newly FTE would have been crossed near the maximum of field aligned current (Figure 4c). On the other hand, the electric and magnetic variations are small in region B and C, which means that the older FTEs would have been crossed far from the maximum field aligned current, that is around the center of the tube. Because FTE footprints are certainly elongated longitudinally (Ref. 31,17), we have chosen the elliptical cross-section model from Wei and Lee (Ref. 32). The magnetic and electric deflections due to a crossing of a footprint of this type are superimposed on Figure 2 in dashed line. The best fit of both Bz and Bx components is obtained for a footprint with a ratio of the major axis to the

minor axis m/n=2.5 and which is crossed in the middle of the upward current side with an angle of 5° between the satellite trajectory and the flow inside the FTE (Figure 2f). In spite of some deviations, the model reproduce quite well the data with a correlation coefficient above 0.9 and a standard deviation around 59 nT. For comparison, the minimum standard deviation obtained for a circular footprint was 40 % larger and for an elliptical footprint with m/n=5, 25 % larger. The characteristics of this FTE deduced from the fit are: a current $i0 \simeq 2 \times 10^4$ A flowing on each edge, a width around 30 km and a length around 80 km. Note that in this idealized model the only currents encountered are located on the edge of the tube and are directed upward (producing a negative gradient of Bz on the edge of the tube and a positive gradient of Bz outside the tube). The model current density at 12:44:26 UT around 26 $\mu A\ m^{-2}$ is a slightly higher than the 18 $\mu A\ m^{-2}$ carried by > 5 eV electrons (deduced from the moments of the electron distribution function). The model Ex and Vram (dashed line in Figure 2c and 2d) has been computed (Ref. 32) using the footprint parameters deduced above and assuming a constant Pedersen conductivity throughout the polar cusp ($\Sigma p = 6.3$). Then these components have been translated along y axis to fit the data. Some deviations are observed between the model and the data, specially on small scales. This could come from the fact that the FTE footprint is not exactly an ellipse or from a variable conductivity through the event due to a variable electron precipitation. Using the conductivity models from Robinson & al (Ref. 33) for the electron precipitation and from Wallis and Budzinski (Ref. 34) for solar illumination, we found Σp around 9 mhos at 12:44:26 UT, which is above the average value taken in our calculation, and Σp around 5 mhos at 12:44:27 UT, which is below the average value. These values would be in agreement with an electric field value smaller than the model at 12:44:26 UT and larger at 12:44:27 UT, which is observed on Figure 2d. Despite these deviations, the model reproduces fairly well the Ex and Vram components and gives a convection inside the FTE $\sim$ 700 m/s. The offset observed between the model and the data, around 15 mV/m for the electric field and -250 m/s for the ram drift, could be due to an offset in the data or to the assumption Σp constant which is not verified. This effect could also be due to the fact that FTE A is produced on a pre-existent flow driven by the previous FTEs B and C (Figure 4).

4. SUMMARY

Three ion energy steps have been observed in a DE 2 cusp crossing. The first step showed a rotation of the flow with a flow directed westward on the equatorward edge, poleward in the center and eastward on the poleward edge. On the other hand the second and third step showed a flow directed principally poleward. In addition, the largest gradients in magnetic field, electric field and convection are observed on the first step and these data are in good agreement with an elongated FTE footprint model. We have interpreted these observations as FTEs injecting particles into the polar ionosphere, the newly reconnected FTE footprint (first step) was crossed on the edge of the event while the two older ones were crossed in the event center. The 3 and 6 min recurrence times of these FTEs are consistent with the small latitudinal size of their footprints ($\sim$40 km) and suggests that an intermittent reconnection with a short recurrence rate could have taken place on the magnetopause.

5. ACKNOWLEDGEMENTS

We gratefully acknowledge N. C. Maynard for providing the DE 2 VEFI data, J. A. Slavin for the MAG-B data and W. B. Hanson for the RPA data. We thank R. M. Candey and N. Reese for their efforts in processing LAPI data. We are grateful to P. T. Newell for helpful discussions. This work was partially supported by CNES under a VSNE contract and by NASA contracts NAGW-1638 and NAS5-31207. CPE was also supported by ESA under a Research Fellowship.

6. REFERENCES

1. Heikkila W J & Winningham J D 1971, Penetration of magnetosheath plasma to low altitudes through the dayside magnetospheric cusps, *J. Geophys. Res.*, 76, 883.

2. Shelley E G & al 1976, He++ and H+ flux measurements in the dayside cusp: estimates of convection electric field, *J. Geophys. Res.*, 81, 2363.

3. Reiff P H & al 1977, Solar wind plasma injection at the dayside magnetospheric cusp, *J. Geophys. Res.*, 82, 479.

4. Reiff P H & al 1980, Cusp proton signatures and the interplanetary magnetic field, *J. Geophys. Res.*, 85, 5997.

5. Escoubet C P & JM Bosqued 1989, The influence of the IMF-Bz and/or AE on the polar cusp: an overview of observations from the AUREOL-3 satellite, *Planet. Space Sci.*, 37, 609.

6. Winningham J D & R A Heelis 1983, The low altitude cleft: Plasma entry and magnetospheric topology, in *High Latitude Space Plasma Physics*, edited by B. Hultqvist and T. Agfors, Plenum, New York, 57.

7. Mukai T & al 1991, Signatures of solar wind injection and transport in the dayside cusp: Exos-D observations, *Geophys. Res. Lett.*, 18, 333.

8. Newell P T & CI Meng 1991, Ion acceleration at the equatorward edge of the cusp: low altitude observations of patchy merging, *Geophys. Res. Lett.*, 18, 1829.

9. Bosqued JM & al 1991, A case study of the cusp electrodynamics by the AUREOL-3 satellite: Evidence of FTE signatures?, *Geophys. Res. Lett.*, 18, 1833.

10. Smiddy M & al 1980, Effects of high-latitude conductivity on observed convection electric fields and Birkeland currents, *J. Geophys. Res.*, 85, 6811.

11. Lockwood M & al, Interplanetary magnetic field control of dayside auroral activity and the transfer of momentum across the dayside magnetopause, *Planet. Space Sci.*, 37, 1347.

12. Carlson C W & R B Torbert 1980, Solar wind injection in the morning auroral oval, *J. Geophys. Res.*, 85, 2903.

13. Russell C T & R C Elphic, ISEE observations of flux transfer events at the dayside magnetopause, *Geophys. Res. Lett.*, 6, 33.

14. Lockwood M & M F Smith, Low-altitude signature of the cusp and flux transfer events, *Geophys. Res. Lett.*, 16, 879.

15. Smith M F & M Lockwood 1990, The pulsating cusp, *Geophys. Res. Lett.*, 17, 1069.

16. Smith M F & al 1992, The statistical cusp: a flux transfer event model, *Planet. Space Sci.*, submitted.

17. Lockwood M & al 1990, The ionospheric signatures of flux transfer events and solar wind dynamic pressure changes, *J. Geophys. Res.*, 95, 17113.

18. Rijnbeek & al 1984, A survey of dayside flux transfer events observed by the ISEE 1 and 2 magnetometers,*J. Geophys. Res.*, 89, 786.

19. Winningham J D & al 1981, The low altitude plasma instrument (LAPI), *Space Sci. Instrum.*, 5, 465-475.

20. Newell P T & CI Meng 1988, The cusp and the cleft/bounda layer: Low-altitude identification and statistical local time variation, *J. Geophys. Res*, 93, 14549.

21. Farthing W H & al 1981, Magnetic field observations on DE-A and -B, *Space Sci. Instrum.*, 5, 465-475.

22. Maynard N C & al 1981, Instrumentation for vector electric field measurements from DE-B, *Space Sci. Instrum.*, 5, 465-475.

23. Sugiura M & al 1984, Relationships between field-aligned currents, electric fields, and particle precipitation as observed by Dynamics Explorer-2, in *Magnetospheric Currents*, edited by T. A. Potemra, AGU, Washington D. C., 96-103.

24. Hanson W B. & al 1981, The Retarding Potential Analyzer for Dynamics Explorer-B, *Space Sci. Instrum.*, 5, 465-475.

25. Menietti J D & JL Burch 1988, Spatial extent of the plasma injection region in the cusp-magnetosheath interface, *J. Geophys. Res.*, 93, 105.

26. Lockwood M & M F Smith 1992, The variation of reconnection rate at the dayside magnetopause and cusp ion precipitation, *J. Geophys. Res.*, submitted.

27. Smith M F & al 1986, Plasma and field observations with high time resolution in flux transfer events, in *Solar Wind-Magnetosphere coupling*, edited by Y. Kamide and J. A. Slavin, Terra Scientific Publishing Company, Tokyo, 321.

28. Cowley S W & al 1991, The ionospheric signatures of flux transfer events, in *Proceedings of the CLUSTER Workshop on Longyearbyen*, ESA SP-330 xxx.

29. Cowley S W & al 1991, Dependence of convective flows and particles precipitation in the high-latitude dayside ionosphere on the X and Y components of the interplanetary magnetic field, *J. Geophys. Res.*, 96, 5557.

30. Crooker N U 1979, Dayside merging and cusp geometry, *J. Geophys. Res.*, 84, 951.

31. Crooker N U & G L Siscoe 1990, On mapping flux transfer events to the ionosphere, *J. Geophys. Res.*, 95, 3795.

32. Wei C Q & L C Lee 1990, Ground magnetic signatures of moving elongated plasma clouds, *J. Geophys. Res.*, 95, 2405.

33. Robinson M R & al 1987, Electrodynamic properties of the evening sector ionosphere within the region 2 field-aligned current sheet, *J. Geophys. Res.*, 92, 731.

34. Wallis D D & E E Budzinski, Empirical models of height integrated conductivities, *J. Geophys. Res.*, 86, 125.